

Predicting Molecular Ground-State Conformation via Conformation Optimization

Fanmeng Wang¹ Minjie Cheng¹ Hongteng Xu^{1,2*}

¹Gaoling School of Artificial Intelligence, Renmin University of China

²Beijing Key Laboratory of Big Data Management and Analysis Methods

October 31, 2024

Abstract

Predicting ground-state conformation from the corresponding molecular graph is crucial for many chemical applications, such as molecular modeling, molecular docking, and molecular property prediction. Recently, many learning-based methods have been proposed to replace time-consuming simulations for this task. However, these methods are often inefficient and sub-optimal as they merely rely on molecular graph information to make predictions from scratch. In this work, considering that molecular low-quality conformations are readily available, we propose a novel framework called ConfOpt to predict molecular ground-state conformation from the perspective of conformation optimization. Specifically, ConfOpt takes the molecular graph and corresponding low-quality 3D conformation as inputs, and then derives the ground-state conformation by iteratively optimizing the low-quality conformation under the guidance of the molecular graph. During training, ConfOpt concurrently optimizes the predicted atomic 3D coordinates and the corresponding interatomic distances, resulting in a strong predictive model. Extensive experiments demonstrate that ConfOpt significantly outperforms existing methods, thus providing a new paradigm for efficiently and accurately predicting molecular ground-state conformation.

1 Introduction

In the past few years, given that molecular interactions are fundamentally three-dimensional [1, 2], molecular modeling has progressed from simple 1D sequences [3, 4] and 2D graphs [5, 6] to crucial 3D structures [7, 8]. While significant progress has been made in various downstream applications like molecular docking [9] and molecular property prediction [10] through incorporating 3D structural information, it has also created a huge demand for scarce high-quality 3D molecular structure data. In this context, molecular ground-state conformation, which represents the most stable 3D molecular structure with the lowest energy and determines many molecular properties [11], becomes increasingly important.

Despite the crucial role that molecular ground-state conformation plays in various downstream applications, obtaining it remains a challenging task [12]. Traditionally, molecular ground-state conformation can be obtained through various experimental or simulation methods. For example, some methods involve molecular dynamics (MD) simulations [13] or density functional theory (DFT) calculations [14] to obtain molecular ground-state conformation. However, these methods like CREST [15] are expensive and computationally slow, thus restricting their ability to meet the growing demands [16]. While some cheminformatics-based prediction methods like RDKit ETKDG [17] have been developed to improve efficiency, they suffer from accuracy shortcomings, which still makes them unsuitable for this task [18]. Given the importance of molecular ground-state conformation and the enormous prediction demands, an ideal method should be able to make both efficient and accurate predictions.

*Corresponding author: Hongteng Xu (hongtengxu@ruc.edu.cn)

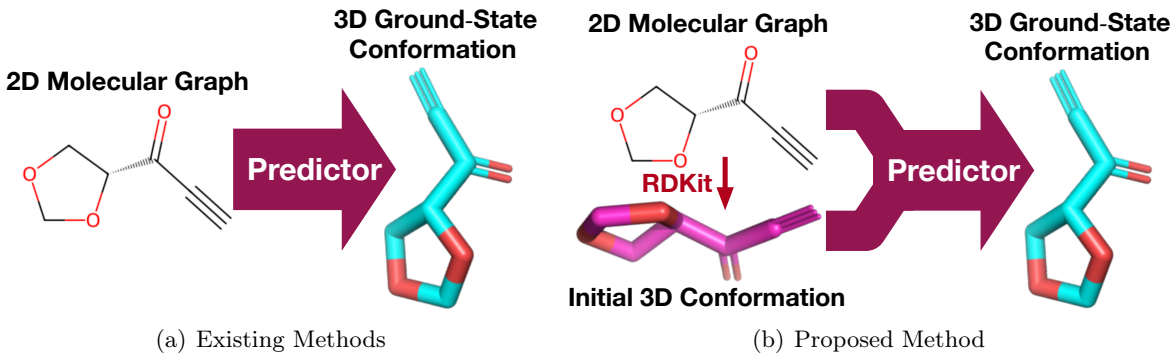


Figure 1: (a) Existing methods only leverage the 2D molecular graph to predict the corresponding ground-state conformation. (b) Our proposed method leverages the 2D graph and the initial 3D conformation generated by RDKit jointly to train a more reliable predictive model.

Recently, with the significant advancement of artificial intelligence in the molecular field, learning-based methods have emerged as a promising solution to tackle this task. Early methods [19, 20] primarily employ various generative models to generate multiple potential low-energy conformations, also known as molecular conformation generation [21]. While easy to implement, these generative methods require additional screening steps to identify the lowest-energy conformation among the generated conformations. Besides, considering the uncertainty of the sampling process, there is no guarantee of sampling the ground-state conformation, further restricting their practical application in the molecular ground-state conformation prediction task [11]. Given the inherent limitations of generative methods, subsequent efforts have started to develop specialized predictive models to determine molecular ground-state conformation directly. Specifically, the work in [22] firstly proposes the Molecule3D benchmark, which comprises approximately 4 million molecules, and develops a deep graph neural network model for the molecular ground-state conformation prediction task. Then the work in [11] further proposes an end-to-end predictive network based on Graph-Transformer to tackle this task and achieve state-of-the-art performance. However, as shown in Figure 1, existing methods only rely on information learned from the corresponding molecular graph to predict molecular ground-state conformation from scratch, still leading to inefficient and sub-optimal performance.

In this work, considering that molecular low-quality conformations are readily available through cheminformatics-based methods such as RDKit ETKDG [17], and various model architectures designed for 3D molecules have made great progress in the past few years [23, 24], we propose a novel framework, called ConfOpt, to predict molecular ground-state conformation from the perspective of conformation optimization. As shown in Figure 2, given the high density of molecular graph information and its importance in guiding the ground-state conformation prediction, our proposed ConfOpt leverages both the molecular graph and the corresponding low-quality conformation as inputs and then iteratively optimizes the low-quality conformation under the guidance of the molecular graph to derive molecular ground-state conformation, thus effectively simplifying the original task and boosting predictive performance. Besides, considering the limitations of previous works that only focus on interatomic distances during training [11], we further introduce a multi-task learning paradigm that concurrently optimizes the predicted atomic 3D coordinates and the corresponding interatomic distances to effectively capture intricate 3D molecular structures, thus enhancing predictive performance in various scenarios.

The extensive experiments consistently demonstrate that our proposed ConfOpt significantly outperforms existing methods and achieves state-of-the-art performance, thus providing a new paradigm for efficiently and accurately predicting molecular ground-state conformation. Comprehensive ablation studies are also conducted to offer valuable insights into the performance of our proposed method, further validating its rationality and effectiveness.

2 Related work

2.1 Molecular Conformation Generation

Molecular conformation generation (MCG) is closely related to molecular ground-state conformation prediction and numerous methods have been proposed in recent years. Specifically, CVGAE [25] is initially introduced to address this task using variational autoencoders [26]. Then CGCF [27] and ConfGF [28] are further proposed to enhance the performance through normalizing flows [29] and score-based generative models [30], respectively. Meanwhile, some works like GeoDiff [31] and TorDiff [32] have leveraged popular diffusion models [33] for generating molecular conformations. Recently, the work in [34] further proposes a gradual optimization learning framework to improve the training of Neural Network Potentials, showing promising outcomes for generating low-energy molecular conformations. However, these methods are essentially designed for obtaining multiple potential low-energy conformations rather than directly obtaining the lowest-energy ground-state conformation [22], necessitating additional screening steps to identify the lowest-energy conformation among the generated conformations when used in the molecular ground-state conformation prediction task. Besides, due to the uncertainty of the sampling process, there is no guarantee of sampling the ground-state conformation, further restricting their practical application in the molecular ground-state conformation prediction task [11].

2.2 Molecular Representation Learning

As the crucial link between large-scale unlabeled molecules and small-scale labeled molecules, molecular representation learning (MRL) has garnered increasing attention in recent years. Initially, inspired by the significant achievements in the area of natural language processing, early works such as SMILES-BERT [3] and Chemberta [4] treat molecules as 1D sequences (e.g., SMILES) and undergo pretraining akin to language models. Then, considering the limited representation capacity of molecular sequences and the rapid development of geometric deep learning [35, 36, 37], molecular representation learning methods based on molecular graphs have become popular. For example, MolCLR [5] involves pretraining on around 10 million molecular graphs through the contrastive learning strategy, leading to notable enhancements in the downstream task. Recently, considering the close correlation between molecular properties and corresponding 3D molecular structure, more and more works are incorporating 3D structural information into pretraining [38, 39]. Specifically, several 3D molecular representation learning methods like Uni-Mol [40] and 3D-PGT [7] have been proposed and shown great capacity in various downstream tasks. With the transition of molecular representation learning to 3D, the demand for scarce high-quality 3D molecular structure data has increased dramatically, thus making it increasingly important to design efficient and accurate molecular ground-state conformation prediction methods.

3 Method

3.1 Preliminary

3.1.1 Notation.

Each molecular graph with n atoms can be denoted as $\mathcal{G} = (\mathcal{V}, \mathcal{E})$, where $\mathcal{V} = \{v_i\}_{i=1}^n$ is the set of vertices representing atoms and $\mathcal{E} = \{e_{ij}\}_{i,j=1}^n$ is the set of edges representing interatomic bonds. Besides, each node $v_i \in \mathcal{V}$ describes the corresponding atomic features (e.g., atomic type, atomic charge, and hybridization state) of i -th atom, while each edge $e_{ij} \in \mathcal{E}$ describes the corresponding bond type (e.g., single, double, triple, aromatic and unconnected) between i -th atom and j -th atom. Moreover, the corresponding ground-state conformation can be denoted as $\mathcal{C} = (\mathcal{A}, \mathcal{P})$, where $\mathcal{A} = [a_i] \in \mathbb{R}^n$ represents atomic types and $\mathcal{P} = [\mathbf{p}_i] \in \mathbb{R}^{n \times 3}$ represents atomic 3D coordinates. In addition, based on the atomic 3D coordinates \mathcal{P} , the corresponding interatomic distances can be denoted as $\mathcal{D} = \{d_{ij}\}_{i,j=1}^n \in \mathbb{R}^{n \times n}$, where $d_{ij} = \|\mathbf{p}_i - \mathbf{p}_j\|_2$ represents the corresponding Euclidean distance between i -th atom and j -th atom in the 3D space.

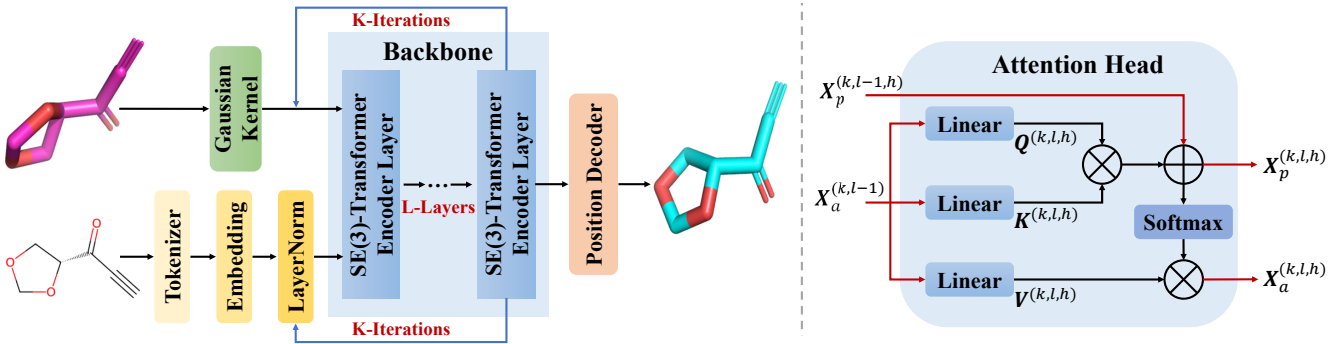


Figure 2: Left: The overall framework of our proposed ConfOpt. Right: The specific implementation of the h -th attention head in the l -th SE(3)-Transformer encoder layer during the k -th iteration.

3.1.2 Problem Definition.

The molecular ground-state conformation prediction task aims to predict the corresponding ground-state conformation $\mathcal{C} = (\mathcal{A}, \mathcal{P})$ from the molecular graph $\mathcal{G} = (\mathcal{V}, \mathcal{E})$. Specifically, considering the atomic type \mathcal{A} is aligned with the vertex set \mathcal{V} , the molecular ground-state conformation prediction task can be further expressed to predict the corresponding atomic 3D coordinates in the ground state from the molecular graph, i.e.,

$$\hat{\mathcal{P}} = \mathcal{M}_\theta(\mathcal{G}) = \mathcal{M}_\theta(\mathcal{V}, \mathcal{E}), \quad (1)$$

where $\hat{\mathcal{P}} = [\hat{\mathbf{p}}_i] \in \mathbb{R}^{n \times 3}$ is the predicted atomic 3D coordinates in the ground state and \mathcal{M}_θ is a ground-state conformation predictive model.

3.1.3 Overview of ConfOpt.

In this work, considering that molecular low-quality conformations are readily available, we propose a novel framework, called ConfOpt, to predict molecular ground-state conformation from the perspective of conformation optimization. As shown in Figure 2, different from previous works that only rely on information learned from the molecular graph to predict the corresponding ground-state conformation from scratch, our proposed ConfOpt also leverages the corresponding low-quality conformation $\tilde{\mathcal{C}}$ generated by RDKit ETKDG [17] as input to provide the initial conformation information. Then under the guidance of the molecular graph \mathcal{G} , ConfOpt iteratively optimizes the corresponding low-quality conformation $\tilde{\mathcal{C}}$ to derive the predicted ground-state conformation $\hat{\mathcal{C}}$, thus effectively simplifying the original molecular ground-state conformation prediction task and boosting predictive performance (see Sec. 3.2 for details). Besides, considering the limitations of previous works that only optimize interatomic distances $\hat{\mathcal{D}}$ acquired from the predicted atomic 3D coordinates $\hat{\mathcal{P}}$ in the training phase, we further propose a multi-task learning paradigm that optimizes both predicted atomic 3D coordinates $\hat{\mathcal{P}}$ and the corresponding interatomic distances $\hat{\mathcal{D}}$ to effectively capture intricate 3D molecular structures, thus enhancing predictive performance in various scenarios. (see Sec. 3.3 for details).

3.2 Model Architecture

3.2.1 Inputs.

As shown in Figure. 2, except for the molecular graph, our proposed ConfOpt also uses the corresponding low-quality conformation $\tilde{\mathcal{C}}$ generated by RDKit ETKDG [17] as input to provide the initial conformation information, thus effectively simplifying the original molecular ground-state conformation prediction task and boosting predictive performance. Then, we further extract the initial atom-level representation $\mathbf{X}_a^{(0,0)}$

and pair-level representations $\mathbf{X}_p^{(0,0)}$ from the molecular graph input \mathcal{G} and corresponding low-quality conformation input $\tilde{\mathcal{C}}$ as inputs of our backbone module, i.e.,

$$\mathbf{X}_a^{(0,0)}, \mathbf{X}_p^{(0,0)} = \epsilon_\theta(\mathcal{G}, \tilde{\mathcal{C}}), \quad (2)$$

where ϵ_θ is the initial representation extraction module.

Here, given the molecular graph \mathcal{G} with n atoms, we first employ the Tokenizer from [6] to extract the chemically meaningful IDs $\mathcal{Z} = [z_i] \in \mathbb{S}^n$ where the vocabulary \mathbb{S} contain $|\mathbb{S}|$ ($|\mathbb{S}| = 512$) discrete codes. These chemically meaningful IDs already contain substantial chemical information about atoms, and previous work [11] has proved that this way can significantly outperform simple Atom-type IDs or traditional Ogb-style IDs [41]. Subsequently, we embed these chemically meaningful IDs as the initial atom-level representation $\mathbf{X}_a^{(0,0)} \in \mathbb{R}^{n \times d_a}$ mentioned in Eq. equation 2 to guide the conformation optimization process. The initial atom-level representation of i -th atom can be obtained as follows:

$$\mathbf{x}_{a,i}^{(0,0)} = f_a(z_i), \quad (3)$$

where f_a embeds each chemically meaningful ID $z_i \in \mathbb{S}$ to the corresponding embedding $\mathbf{x}_{a,i}^{(0,0)} \in \mathbb{R}^{d_a}$.

Meanwhile, with the corresponding low-quality conformation $\tilde{\mathcal{C}}$, we use the pair-type aware Gaussian kernel function [42] to transform the Euclidean distances among atom pairs into the initial pair-level representation $\mathbf{X}_p^{(0,0)} \in \mathbb{R}^{n \times n \times d_p}$ mentioned in Eq. equation 2 to provide the initial conformation information. The initial pair-level representation of atom pair (i, j) can be obtained as follows:

$$\mathbf{x}_{p,ij}^{(0,0)} = \mathcal{G}(\mathbf{u}_{\tilde{a}_i \tilde{a}_j} \|\tilde{\mathbf{p}}_i - \tilde{\mathbf{p}}_j\|_2 + \mathbf{v}_{\tilde{a}_i \tilde{a}_j} - \boldsymbol{\mu}, \boldsymbol{\sigma}), \quad (4)$$

where \mathcal{G} is a predefined Gaussian kernel function with mean value $\boldsymbol{\mu} \in \mathbb{R}^{d_p}$ and standard deviation $\boldsymbol{\sigma} \in \mathbb{R}^{d_p}$, $\mathbf{u}_{\tilde{a}_i \tilde{a}_j} \in \mathbb{R}^{d_p}$ and $\mathbf{v}_{\tilde{a}_i \tilde{a}_j} \in \mathbb{R}^{d_p}$ represent the weights and biases which are learnable parameters for each atom type pair $(\tilde{a}_i, \tilde{a}_j)$, and $\|\tilde{\mathbf{p}}_i - \tilde{\mathbf{p}}_j\|_2$ represents the corresponding Euclidean distance between i -th atom and j -th atom in the 3D space.

3.2.2 Backbone.

After extracting the initial atom-level representation $\mathbf{X}_a^{(0,0)}$ and pair-level representations $\mathbf{X}_p^{(0,0)}$, we use the backbone module ϕ_θ , which is composed of L SE(3)-Transformer encoder layers [23], to iteratively optimize the low-quality conformation information under the guidance of the information learned from the molecular graph, thus deriving the final atom-level representation $\mathbf{X}_a^{(K,L)}$ and pair-level representation $\mathbf{X}_p^{(K,L)}$, i.e.,

$$\mathbf{X}_a^{(K,L)}, \mathbf{X}_p^{(K,L)} = \phi_\theta^K(\mathbf{X}_a^{(0,0)}, \mathbf{X}_p^{(0,0)}), \quad (5)$$

where K is the number of iterations. During the i -th iteration, our backbone module ϕ_θ takes the representation $\mathbf{X}_a^{(i,0)}$ and $\mathbf{X}_p^{(i,0)}$ as inputs and process them through L SE(3)-Transformer encoder layers to obtain the output representations $\mathbf{X}_a^{(i,L)}$ and $\mathbf{X}_p^{(i,L)}$, which are also used as the inputs of the next iteration.

To effectively capture intricate 3D structure information and optimize the low-quality conformation, the atom-to-pair communication [40] is utilized in the SE(3)-Transformer encoder layer to improve the traditional self-attention mechanism. As shown in Figure. 2, the specific implementation of the h -th attention head in the l -th SE(3)-Transformer encoder layer during the k -th iteration can be expressed as follows:

$$\begin{aligned} \mathbf{A}^{(k,l,h)} &= \frac{\mathbf{Q}^{(k,l,h)}(\mathbf{K}^{(k,l,h)})^\top}{\sqrt{d_h}} + \mathbf{X}_p^{(k,l-1,h)}, \\ \mathbf{X}_a^{(k,l,h)} &= \sigma(\mathbf{A}^{(k,l,h)})\mathbf{V}^{(k,l,h)}, \quad \mathbf{X}_p^{(k,l,h)} = \mathbf{A}^{(k,l,h)}, \end{aligned} \quad (6)$$

where $\mathbf{Q}^{(k,l,h)}$, $\mathbf{K}^{(k,l,h)}$, and $\mathbf{V}^{(k,l,h)} \in \mathbb{R}^{n \times d_h}$ are the query, key, and value matrices derived by applying the corresponding linear maps $\mathbf{W}_Q^{(l,h)}$, $\mathbf{W}_K^{(l,h)}$, and $\mathbf{W}_V^{(l,h)} \in \mathbb{R}^{d_a \times d_h}$ to the input $\mathbf{X}_a^{(k,l-1)} \in \mathbb{R}^{n \times d_a}$. Besides,

$d_h = d_a/d_p$ is the hidden dimension of each attention head, $\mathbf{X}_p^{(k,l-1,h)} \in \mathbb{R}^{n \times n}$ is the h -th slice of the input $\mathbf{X}_p^{(k,l-1)} \in \mathbb{R}^{n \times n \times d_p}$, and $\sigma(\cdot)$ is the row-wise softmax operator.

Through L SE(3)-Transformer encoder layers and K iterations, we can obtain the final representation outputs $\mathbf{X}_a^{(K,L)}$ and $\mathbf{X}_p^{(K,L)}$ mentioned in Eq. equation 5 as follows:

$$\begin{aligned}\mathbf{X}_a^{(K,L)} &= \text{Concat}(\{\mathbf{X}_a^{(K,L,h)}\}_{h=1}^{d_p}) \mathbf{W}_O + \mathbf{X}_a^{(K,L-1)}, \\ \mathbf{X}_p^{(K,L)} &= \text{Concat}(\{\mathbf{X}_p^{(K,L,h)}\}_{h=1}^{d_p}),\end{aligned}\quad (7)$$

where $\text{Concat}(\cdot)$ is the concatenation operator, and $\mathbf{W}_O \in \mathbb{R}^{d_a \times d_a}$ is the feed-forward neural network.

3.2.3 Position Decoder.

Finally, we use a pair-level position decoder ψ_θ to decode the predicted atomic 3D coordinates $\hat{\mathcal{P}}$ in the ground-state conformation $\hat{\mathcal{C}}$ from the inputs and outputs of the backbone module along with the atomic 3D coordinates $\tilde{\mathcal{P}}$ in the input low-quality conformation $\tilde{\mathcal{C}}$, i.e.,

$$\hat{\mathcal{P}} = \psi_\theta(\tilde{\mathcal{P}}, \mathbf{X}_p^{(0,0)}, \mathbf{X}_p^{(K,L)}). \quad (8)$$

Here, based on the pair-level position decoder ψ_θ , the specific calculation of the corresponding 3D coordinate in the ground state for i -th atom can be expressed as follows:

$$\hat{\mathbf{p}}_i = \tilde{\mathbf{p}}_i + \sum_{j=1}^n \frac{f_p(\mathbf{x}_{p,ij}^{(K,L)} - \mathbf{x}_{p,ij}^{(0,0)}) (\tilde{\mathbf{p}}_i - \tilde{\mathbf{p}}_j)}{n}, \quad (9)$$

where $\hat{\mathbf{p}}_i \in \mathbb{R}^3$ is the predicted 3D coordinate of i -th atom in the ground-state conformation $\hat{\mathcal{C}}$ and $\tilde{\mathbf{p}}_i \in \mathbb{R}^3$ is the 3D coordinate of i -th atom in the input low-quality conformation $\tilde{\mathcal{C}}$. Besides, n is the number of atoms, and $f_p(\cdot)$ is an MLP layer that maps the updated pair-level representation $(\mathbf{x}_{p,ij}^{(K,L)} - \mathbf{x}_{p,ij}^{(0,0)}) \in \mathbb{R}^{d_p}$ of atom pair (i, j) to a scalar as the weight of the corresponding displacement vectors.

3.3 Learning Paradigm

As mentioned earlier, the molecular ground-state conformation prediction task aims to predict the corresponding 3D coordinate in the ground state for each atom in the molecule. However, previous works only constrain the interatomic distances $\hat{\mathcal{D}}$ acquired from the predicted atomic 3D coordinates $\hat{\mathcal{P}}$ during training, thus seriously limiting their performance.

Here, to overcome the limitations of previous works, we further propose a multi-task learning paradigm that constrains both predicted atomic 3D coordinates $\hat{\mathcal{P}}$ and the corresponding interatomic distances $\hat{\mathcal{D}}$ to enhance predictive performance in various scenarios.

Specifically, given the predicted atomic 3D coordinates $\hat{\mathcal{P}}$ and corresponding ground truth \mathcal{P} , we firstly align \mathcal{P} to $\hat{\mathcal{P}}$ in the 3D space i.e.,

$$\begin{aligned}\mathcal{P}_0 &= \mathcal{P} - \frac{1}{n} \sum_{i=1}^n \mathbf{p}_i, \quad \hat{\mathcal{P}}_0 = \hat{\mathcal{P}} - \frac{1}{n} \sum_{i=1}^n \hat{\mathbf{p}}_i, \\ \mathcal{P}^* &= \text{Align}(\mathcal{P}_0, \hat{\mathcal{P}}_0) = \mathcal{P}_0 \text{Rot}(\mathcal{P}_0, \hat{\mathcal{P}}_0) = \mathcal{P}_0 \mathbf{V} \mathbf{U}^T,\end{aligned}\quad (10)$$

where \mathcal{P}_0 and $\hat{\mathcal{P}}_0$ are zero-mean atomic 3D coordinates, and \mathcal{P}^* is the aligned ground truth. $\text{Rot}(\mathcal{P}_0, \hat{\mathcal{P}}_0)$ is the rotation matrix derived by Procrustes analysis [43], in which \mathbf{U} and \mathbf{V} are obtained from the singular value decomposition (SVD) of $\hat{\mathcal{P}}_0^T \mathcal{P}_0$.

Subsequently, we use the MAE loss [44] as our loss function to constrain both predicted atomic 3D coordinates $\hat{\mathcal{P}}$ and the corresponding interatomic distances $\hat{\mathcal{D}}$ during training as follows:

$$\mathcal{L} = \underbrace{\text{MAE}(\hat{\mathcal{P}}, \mathcal{P}^*)}_{\mathcal{L}_{\text{coord}}} + \lambda \underbrace{\text{MAE}(\hat{\mathcal{D}}, \mathcal{D}^*)}_{\mathcal{L}_{\text{distan}}}, \quad (11)$$

where λ is the weight of the interatomic distance loss.

The whole learning paradigm can be expressed in algorithm 1. Besides, we can apply the learned ConfOpt to predict atomic 3D coordinates $\hat{\mathcal{P}}$ in the ground state (the atomic types \mathcal{A} can be obtained directly from the molecular graph input \mathcal{G}) as details in algorithm 2.

Algorithm 1 Training.

Require: $\mathcal{G}, \tilde{\mathcal{P}}, \mathcal{P}, \epsilon_\theta, \phi_\theta, \psi_\theta$

```

1: # Initial representation extraction
2:  $\mathbf{X}_a^{(0,0)}, \mathbf{X}_p^{(0,0)} = \epsilon_\theta(\mathcal{G}, \tilde{\mathcal{C}})$ 
3: # Iterative representation optimization
4: for  $k = 0, 1, \dots, K$  do
5:    $\mathbf{X}_a^{(k,L)}, \mathbf{X}_p^{(k,L)} = \phi_\theta(\mathbf{X}_a^{(k,0)}, \mathbf{X}_p^{(k,0)})$ 
6:    $\mathbf{X}_a^{(k+1,0)}, \mathbf{X}_p^{(k+1,0)} = \mathbf{X}_a^{(k,L)}, \mathbf{X}_p^{(k,L)}$ 
7: end for
8: # Position decoding
9:  $\hat{\mathcal{P}} = \psi_\theta(\tilde{\mathcal{P}}, \mathbf{X}_p^{(0,0)}, \mathbf{X}_p^{(K,L)})$ 
10: # Loss calculation
11:  $\mathcal{P}_0 = \mathcal{P} - \frac{1}{n} \sum_{i=1}^n \mathbf{p}_i, \quad \hat{\mathcal{P}}_0 = \hat{\mathcal{P}} - \frac{1}{n} \sum_{i=1}^n \hat{\mathbf{p}}_i$ 
12:  $\mathcal{P}^* = \text{Align}(\mathcal{P}_0, \hat{\mathcal{P}}_0)$ 
13:  $\mathcal{L} = \text{MAE}(\hat{\mathcal{P}}, \mathcal{P}^*) + \lambda \text{MAE}(\hat{\mathcal{D}}, \mathcal{D}^*)$ 
14: #  $\theta$  optimization with  $\mathcal{L}$  over batch
15:  $\theta = \text{Adam}(\mathcal{L}, \epsilon_\theta, \phi_\theta, \psi_\theta)$ 
16: return  $\theta$ 

```

Algorithm 2 Inference.

Require: $\mathcal{G}, \tilde{\mathcal{P}}, \epsilon_\theta, \phi_\theta, \psi_\theta$

```

1: # Initial representation extraction
2:  $\mathbf{X}_a^{(0,0)}, \mathbf{X}_p^{(0,0)} = \epsilon_\theta(\mathcal{G}, \tilde{\mathcal{C}})$ 
3: # Iterative representation optimization
4: for  $k = 0, 1, \dots, K$  do
5:    $\mathbf{X}_a^{(k,L)}, \mathbf{X}_p^{(k,L)} = \phi_\theta(\mathbf{X}_a^{(k,0)}, \mathbf{X}_p^{(k,0)})$ 
6:    $\mathbf{X}_a^{(k+1,0)}, \mathbf{X}_p^{(k+1,0)} = \mathbf{X}_a^{(k,L)}, \mathbf{X}_p^{(k,L)}$ 
7: end for
8: # Position decoding
9:  $\hat{\mathcal{P}} = \psi_\theta(\tilde{\mathcal{P}}, \mathbf{X}_p^{(0,0)}, \mathbf{X}_p^{(K,L)})$ 
10: return Atomic coordinates  $\hat{\mathcal{P}}$  in the ground state

```

4 Experiments

4.1 Experimental Setup

4.1.1 Datasets.

Following previous works, we also employ the Molecule3D and QM9 datasets to validate the effectiveness of our proposed method:

- **Molecule3D.** The first benchmark introduced by [22] for the molecular ground-state conformation prediction task. It comprises approximately 4 million molecules, each with its corresponding ground-state conformation calculated by DFT. Besides, it provides two dataset-splitting results (i.e., random and scaffold splitting) to ensure a comprehensive evaluation.
- **QM9.** A small-scale quantum chemistry dataset introduced by [11] for the molecular ground-state conformation prediction task. It comprises approximately 130,000 molecules with 9 heavy atoms, each with its corresponding ground-state conformation calculated by DFT. Besides, it adopts the identical dataset-splitting strategy described in [45].

4.1.2 Evaluation metircs.

To guarantee a comprehensive and fair assessment, we choose the same metrics introduced by [11], including D-MAE, D-RMSE, and C-RMSD to evaluate the predictive performance in terms of interatomic distances

Table 1: The performance of different methods on the Molecule3D and QM9 datasets

Dataset	Splitting	Method	Valid			Test		
			D-MAE ↓	D-RMSE ↓	C-RMSD ↓	D-MAE ↓	D-RMSE ↓	C-RMSD ↓
Molecule3D	Random	RDKit ETKDG	0.575	0.941	0.998	0.576	0.942	0.999
		GINE	0.590	1.014	1.116	0.592	1.018	1.116
		GATv2	0.563	0.983	1.082	0.564	0.986	1.083
		GPS	0.528	0.909	1.036	0.529	0.911	1.038
		GTMGC	0.432	0.719	0.712	0.433	0.721	0.713
		ConfOpt-3D	0.651	0.938	0.772	0.652	0.940	0.773
		ConfOpt (Ours)	0.420	0.700	0.696	0.421	0.703	0.697
	Scaffold	RDKit ETKDG	0.531	0.874	0.928	0.511	0.859	0.898
		GINE	0.883	1.517	1.407	1.400	2.224	1.960
		GATv2	0.778	1.385	1.254	1.238	2.069	1.752
		GPS	0.538	0.885	1.031	0.657	1.091	1.136
		GTMGC	0.406	0.675	0.678	0.400	0.679	0.693
		ConfOpt-3D	0.618	0.896	0.734	0.610	0.890	0.732
		ConfOpt (Ours)	0.394	0.658	0.666	0.393	0.674	0.685
QM9	Default	RDKit ETKDG	0.355	0.621	0.691	0.355	0.621	0.689
		GINE	0.357	0.673	0.685	0.357	0.669	0.693
		GATv2	0.339	0.663	0.661	0.339	0.659	0.666
		GPS	0.326	0.644	0.662	0.326	0.640	0.666
		GTMGC	0.262	0.468	0.362	0.264	0.470	0.367
		ConfOpt-3D	0.340	0.563	0.252	0.343	0.565	0.258
		ConfOpt (Ours)	0.233	0.425	0.202	0.237	0.432	0.212

* ConfOpt-3D refers to directly optimizing the low-quality conformation without the guidance of the corresponding molecular graph.

and atomic 3D coordinates. The specific calculation of these metrics is as follows:

$$\text{D-MAE}(\hat{\mathcal{D}}, \mathcal{D}^*) = \frac{1}{n^2} \sum_{i=1}^n \sum_{j=1}^n |\hat{d}_{ij} - d_{ij}^*|, \quad (12)$$

$$\text{D-RMSE}(\hat{\mathcal{D}}, \mathcal{D}^*) = \sqrt{\frac{1}{n^2} \sum_{i=1}^n \sum_{j=1}^n (\hat{d}_{ij} - d_{ij}^*)^2}, \quad (13)$$

$$\text{C-RMSD}(\hat{\mathcal{P}}, \mathcal{P}^*) = \sqrt{\frac{1}{n} \sum_{i=1}^n \|\hat{\mathbf{p}}_i - \mathbf{p}_i^*\|_2^2}. \quad (14)$$

4.1.3 Baselines.

To fully demonstrate the effectiveness of our proposed method, we compare our proposed method with the state-of-the-art method GTMGC [11] and its typical baselines, including RDKit ETKDG [17], GINE [46], GATv2 [47] and GPS [48].

4.2 Comparison

Table 1 summarizes the performance of different methods on the Molecule3D and QM9 datasets, which are evaluated by D-MAE, D-RMSE, and C-RMSD together. As shown in this table, our proposed method, ConfOpt, significantly outperforms all baselines across all evaluation metrics on all datasets, achieving state-of-the-art performance.

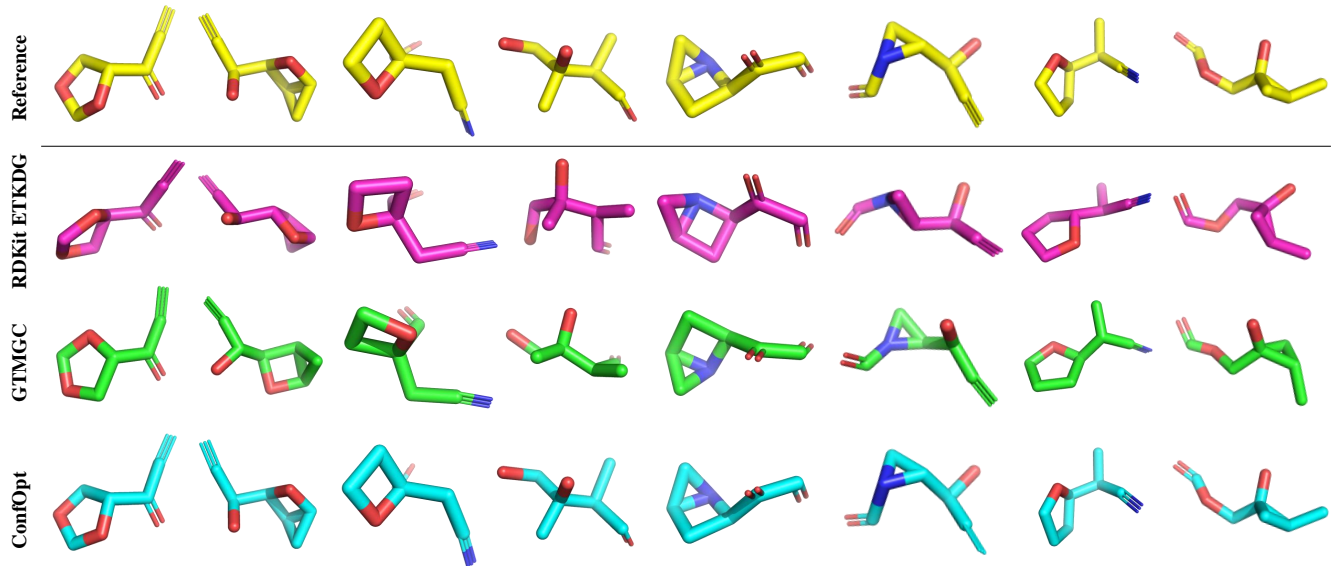


Figure 3: Several molecular ground-state conformation prediction results of RDKit ETKDG (the input low-quality conformation), GTMGC (the best baseline), and our proposed ConfOpt.

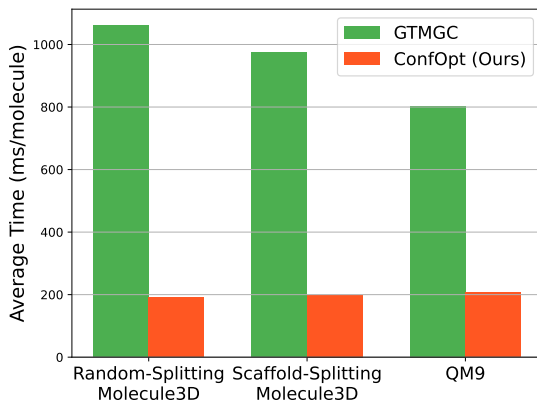


Figure 4: Efficiency comparison between GTMGC (the best baseline) and our proposed ConfOpt.

Specifically, the comparison with ConfOpt-3D demonstrates the crucial role of molecular graph information in predicting molecular ground-state conformation, especially for large molecules (i.e., Molecule3D dataset), thus proving the rationality of our proposed ConfOpt optimizing the low-quality conformation under the guidance of the corresponding molecular graph. Besides, the very close results of our proposed ConfOpt on the valid set and test set across all datasets also highlight its great generalization capacity.

In addition, we visualize several samples predicted by various methods in Figure. 3 to provide a qualitative comparison. As shown in this figure, compared with the prediction results of RDKit ETKDG (the input low-quality conformation) and GTMGC (the best baseline), the ground-state conformations predicted by our proposed ConfOpt align more closely with the references, further proving its superiority on the molecular ground-state conformation prediction task.

Moreover, Figure. 4 also compares the efficiency of GTMGC (the best baseline) and our proposed ConfOpt by calculating the average time taken per molecule on each dataset. As shown in Figure. 4 and Table 1, our proposed ConfOpt can significantly decrease the average time taken per molecule by over 70% while enhancing predictive performance across all datasets. In this way, our proposed ConfOpt successfully achieves both efficient and accurate molecular ground-state conformation prediction, showing its great potential for tackling this task.

Table 2: The performance of our proposed ConfOpt under different learning paradigms

Dataset	Splitting	Training Setting		Valid			Test		
		\mathcal{L}_{coord}	\mathcal{L}_{distan}	D-MAE \downarrow	D-RMSE \downarrow	C-RMSD \downarrow	D-MAE \downarrow	D-RMSE \downarrow	C-RMSD \downarrow
Molecule3D	Random	✓	✗	0.681	0.968	0.798	0.681	0.969	0.799
		✗	✓	0.421	0.705	0.743	0.423	0.708	0.744
		✓	✓	0.420	0.700	0.696	0.421	0.703	0.697
	Scaffold	✓	✗	0.630	0.905	0.764	0.620	0.898	0.765
		✗	✓	0.395	0.661	0.716	0.394	0.679	0.725
		✓	✓	0.394	0.658	0.666	0.393	0.674	0.685
QM9	Default	✓	✗	0.347	0.565	0.276	0.348	0.566	0.283
		✗	✓	0.244	0.447	0.286	0.247	0.452	0.291
		✓	✓	0.233	0.425	0.202	0.237	0.432	0.212

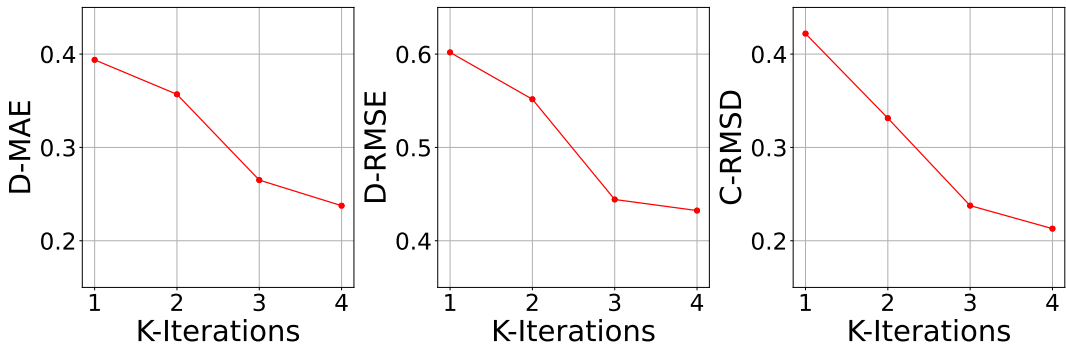


Figure 5: The performance of our proposed ConfOpt on the QM9 dataset under different iterations.

4.3 Effectiveness Analysis

As illustrated in Sec. 3.3, different from previous works that only optimize the interatomic distances, we further propose a multi-task learning paradigm, which constrains predicted atomic 3D coordinates and the corresponding interatomic distances together during training, to enhance predictive performance. Table 2 displays the performance of our proposed ConfOpt on the Molecule3D and QM9 datasets under different learning paradigms to evaluate the rationality and effectiveness of our proposed multi-task learning paradigm. On the one hand, in most cases, merely constraining predicted atomic 3D coordinates performs significantly worse than constraining the corresponding interatomic distances. This phenomenon aligns with previous works prioritizing constraining corresponding interatomic distances over predicted atomic 3D coordinates, proving the importance of focusing on corresponding interatomic distances during training. On the other hand, compared with merely constraining one term (either predicted atomic 3D coordinates or corresponding interatomic distances), constraining them together during training can achieve better performance across all evaluation metrics on all datasets, thus greatly supporting the rationality and effectiveness of our proposed multi-task learning paradigm.

In addition, as our proposed ConfOpt derives the molecular ground-state conformation by iteratively optimizing the low-quality conformation, we further analyze its performance under different iterations to validate the rationality and effectiveness of the conformation iterative optimization. As shown in Figure 5, the performance of our proposed ConfOpt improves steadily and gradually converges with more iterations, thus proving that our proposed ConfOpt can effectively employ conformation iterative optimization to derive the ground-state conformation.

5 Conclusion

In this work, we present ConfOpt, a novel framework that effectively simplifies and tackles the molecular ground-state conformation prediction task from the perspective of conformation optimization. Meanwhile, we introduce a multi-task learning paradigm that concurrently optimizes the predicted atomic 3D coordinates and the corresponding interatomic distances during training to improve predictive performance in various scenarios. Extensive experiments demonstrate that our proposed ConfOpt can significantly outperform existing methods and achieve state-of-the-art performance, thus providing a new paradigm for efficiently and accurately predicting molecular ground-state conformation.

References

- [1] J. Zhu, Y. Xia, L. Wu, S. Xie, T. Qin, W. Zhou, H. Li, and T.-Y. Liu, “Unified 2d and 3d pre-training of molecular representations,” in *Proceedings of the 28th ACM SIGKDD conference on knowledge discovery and data mining*, 2022, pp. 2626–2636.
- [2] F. Wang, H. Xu, X. Chen, S. Lu, Y. Deng, and W. Huang, “Mperformer: An se (3) transformer-based molecular perceptron,” in *Proceedings of the 32nd ACM International Conference on Information and Knowledge Management*, 2023, pp. 2512–2522.
- [3] S. Wang, Y. Guo, Y. Wang, H. Sun, and J. Huang, “Smiles-bert: large scale unsupervised pre-training for molecular property prediction,” in *Proceedings of the 10th ACM international conference on bioinformatics, computational biology and health informatics*, 2019, pp. 429–436.
- [4] S. Chithrananda, G. Grand, and B. Ramsundar, “Chemberta: large-scale self-supervised pretraining for molecular property prediction,” *arXiv preprint arXiv:2010.09885*, 2020.
- [5] Y. Wang, J. Wang, Z. Cao, and A. Barati Farimani, “Molecular contrastive learning of representations via graph neural networks,” *Nature Machine Intelligence*, vol. 4, no. 3, pp. 279–287, 2022.
- [6] J. Xia, C. Zhao, B. Hu, Z. Gao, C. Tan, Y. Liu, S. Li, and S. Z. Li, “Mole-bert: Rethinking pre-training graph neural networks for molecules,” in *The Eleventh International Conference on Learning Representations*, 2022.
- [7] X. Wang, H. Zhao, W.-w. Tu, and Q. Yao, “Automated 3d pre-training for molecular property prediction,” in *Proceedings of the 29th ACM SIGKDD Conference on Knowledge Discovery and Data Mining*, 2023, pp. 2419–2430.
- [8] R. Jiao, J. Han, W. Huang, Y. Rong, and Y. Liu, “Energy-motivated equivariant pretraining for 3d molecular graphs,” in *Proceedings of the AAAI Conference on Artificial Intelligence*, vol. 37, no. 7, 2023, pp. 8096–8104.
- [9] A. Chatterjee, R. Walters, Z. Shafi, O. S. Ahmed, M. Sebek, D. Gysi, R. Yu, T. Eliassi-Rad, A.-L. Barabási, and G. Menichetti, “Improving the generalizability of protein-ligand binding predictions with ai-bind,” *Nature communications*, vol. 14, no. 1, p. 1989, 2023.
- [10] K. Moon, H.-J. Im, and S. Kwon, “3d graph contrastive learning for molecular property prediction,” *Bioinformatics*, vol. 39, no. 6, p. btad371, 2023.
- [11] G. Xu, Y. Jiang, P. Lei, Y. Yang, and J. Chen, “Gtmgc: Using graph transformer to predict molecule’s ground-state conformation,” in *The Twelfth International Conference on Learning Representations*, 2023.
- [12] P. C. Hawkins, “Conformation generation: the state of the art,” *Journal of chemical information and modeling*, vol. 57, no. 8, pp. 1747–1756, 2017.

- [13] O. M. Salo-Ahen, I. Alanko, R. Bhadane, A. M. Bonvin, R. V. Honorato, S. Hossain, A. H. Juffer, A. Kabedev, M. Lahtela-Kakkonen, A. S. Larsen *et al.*, “Molecular dynamics simulations in drug discovery and pharmaceutical development,” *Processes*, vol. 9, no. 1, p. 71, 2020.
- [14] D. S. Sholl and J. A. Steckel, *Density functional theory: a practical introduction*. John Wiley & Sons, 2022.
- [15] P. Pracht, F. Bohle, and S. Grimme, “Automated exploration of the low-energy chemical space with fast quantum chemical methods,” *Physical Chemistry Chemical Physics*, vol. 22, no. 14, pp. 7169–7192, 2020.
- [16] S. Axelrod and R. Gomez-Bombarelli, “Geom, energy-annotated molecular conformations for property prediction and molecular generation,” *Scientific Data*, vol. 9, no. 1, p. 185, 2022.
- [17] S. Riniker and G. A. Landrum, “Better informed distance geometry: using what we know to improve conformation generation,” *Journal of chemical information and modeling*, vol. 55, no. 12, pp. 2562–2574, 2015.
- [18] D. Reidenbach and A. Krishnapriyan, “Coarsenconf: Equivariant coarsening with aggregated attention for molecular conformer generation,” in *NeurIPS 2023 Generative AI and Biology (GenBio) Workshop*, 2023.
- [19] M. Xu, W. Wang, S. Luo, C. Shi, Y. Bengio, R. Gomez-Bombarelli, and J. Tang, “An end-to-end framework for molecular conformation generation via bilevel programming,” in *International conference on machine learning*. PMLR, 2021, pp. 11 537–11 547.
- [20] O. Ganea, L. Pattanaik, C. Coley, R. Barzilay, K. Jensen, W. Green, and T. Jaakkola, “Geomol: Torsional geometric generation of molecular 3d conformer ensembles,” *Advances in Neural Information Processing Systems*, vol. 34, pp. 13 757–13 769, 2021.
- [21] G. Zhou, Z. Gao, Z. Wei, H. Zheng, and G. Ke, “Do deep learning methods really perform better in molecular conformation generation?” in *ICLR 2023-Machine Learning for Drug Discovery workshop*, 2023.
- [22] Z. Xu, Y. Luo, X. Zhang, X. Xu, Y. Xie, M. Liu, K. Dickerson, C. Deng, M. Nakata, and S. Ji, “Molecule3d: A benchmark for predicting 3d geometries from molecular graphs,” *arXiv preprint arXiv:2110.01717*, 2021.
- [23] F. Fuchs, D. Worrall, V. Fischer, and M. Welling, “Se (3)-transformers: 3d roto-translation equivariant attention networks,” *Advances in neural information processing systems*, vol. 33, pp. 1970–1981, 2020.
- [24] Y.-L. Liao and T. Smidt, “Equiformer: Equivariant graph attention transformer for 3d atomistic graphs,” in *The Eleventh International Conference on Learning Representations*, 2022.
- [25] E. Mansimov, O. Mahmood, S. Kang, and K. Cho, “Molecular geometry prediction using a deep generative graph neural network,” *Scientific reports*, vol. 9, no. 1, p. 20381, 2019.
- [26] D. P. Kingma and M. Welling, “Auto-encoding variational bayes,” *arXiv preprint arXiv:1312.6114*, 2013.
- [27] M. Xu, S. Luo, Y. Bengio, J. Peng, and J. Tang, “Learning neural generative dynamics for molecular conformation generation,” *arXiv preprint arXiv:2102.10240*, 2021.
- [28] C. Shi, S. Luo, M. Xu, and J. Tang, “Learning gradient fields for molecular conformation generation,” in *International conference on machine learning*. PMLR, 2021, pp. 9558–9568.

[29] I. Kobyzev, S. J. Prince, and M. A. Brubaker, “Normalizing flows: An introduction and review of current methods,” *IEEE transactions on pattern analysis and machine intelligence*, vol. 43, no. 11, pp. 3964–3979, 2020.

[30] Y. Song, J. Sohl-Dickstein, D. P. Kingma, A. Kumar, S. Ermon, and B. Poole, “Score-based generative modeling through stochastic differential equations,” in *International Conference on Learning Representations*, 2020.

[31] M. Xu, L. Yu, Y. Song, C. Shi, S. Ermon, and J. Tang, “Geodiff: A geometric diffusion model for molecular conformation generation,” in *International Conference on Learning Representations*, 2021.

[32] B. Jing, G. Corso, J. Chang, R. Barzilay, and T. Jaakkola, “Torsional diffusion for molecular conformer generation,” *Advances in Neural Information Processing Systems*, vol. 35, pp. 24 240–24 253, 2022.

[33] J. Ho, A. Jain, and P. Abbeel, “Denoising diffusion probabilistic models,” *Advances in neural information processing systems*, vol. 33, pp. 6840–6851, 2020.

[34] A. Tsypin, L. A. Ugadiarov, K. Khrabrov, A. Telepov, E. Rumiantsev, A. Skrynnik, A. Panov, D. P. Vetrov, E. Tutubalina, and A. Kadurin, “Gradual optimization learning for conformational energy minimization,” in *The Twelfth International Conference on Learning Representations*, 2024. [Online]. Available: <https://openreview.net/forum?id=FMMF1a9ifL>

[35] J. Han, Y. Rong, T. Xu, and W. Huang, “Geometrically equivariant graph neural networks: A survey,” *arXiv preprint arXiv:2202.07230*, 2022.

[36] W. Ju, Z. Fang, Y. Gu, Z. Liu, Q. Long, Z. Qiao, Y. Qin, J. Shen, F. Sun, Z. Xiao *et al.*, “A comprehensive survey on deep graph representation learning,” *Neural Networks*, p. 106207, 2024.

[37] J. Cen, A. Li, N. Lin, Y. Ren, Z. Wang, and W. Huang, “Are high-degree representations really unnecessary in equivariant graph neural networks?” in *The Thirty-eighth Annual Conference on Neural Information Processing Systems*, 2024. [Online]. Available: <https://openreview.net/forum?id=M0ncNVuGYN>

[38] S. Liu, H. Wang, W. Liu, J. Lasenby, H. Guo, and J. Tang, “Pre-training molecular graph representation with 3d geometry,” in *International Conference on Learning Representations*, 2021.

[39] F. Wang, W. Guo, M. Cheng, S. Yuan, H. Xu, and Z. Gao, “Mmpolymer: A multimodal multitask pretraining framework for polymer property prediction,” in *Proceedings of the 33rd ACM International Conference on Information and Knowledge Management*, 2024, pp. 2336–2346.

[40] G. Zhou, Z. Gao, Q. Ding, H. Zheng, H. Xu, Z. Wei, L. Zhang, and G. Ke, “Uni-mol: A universal 3d molecular representation learning framework,” in *The Eleventh International Conference on Learning Representations*, 2022.

[41] W. Hu, M. Fey, H. Ren, M. Nakata, Y. Dong, and J. Leskovec, “Ogb-lsc: A large-scale challenge for machine learning on graphs,” in *Thirty-fifth Conference on Neural Information Processing Systems Datasets and Benchmarks Track (Round 2)*, 2021.

[42] B. Scholkopf, K.-K. Sung, C. J. Burges, F. Girosi, P. Niyogi, T. Poggio, and V. Vapnik, “Comparing support vector machines with gaussian kernels to radial basis function classifiers,” *IEEE transactions on Signal Processing*, vol. 45, no. 11, pp. 2758–2765, 1997.

[43] C. Wang and S. Mahadevan, “Manifold alignment using procrustes analysis,” in *Proceedings of the 25th international conference on Machine learning*, 2008, pp. 1120–1127.

- [44] Q. Wang, Y. Ma, K. Zhao, and Y. Tian, “A comprehensive survey of loss functions in machine learning,” *Annals of Data Science*, pp. 1–26, 2020.
- [45] Y.-L. Liao and T. Smidt, “Equiformer: Equivariant graph attention transformer for 3d atomistic graphs,” in *International Conference on Learning Representations*, 2023. [Online]. Available: <https://openreview.net/forum?id=KwmPfARgOTD>
- [46] W. Hu, B. Liu, J. Gomes, M. Zitnik, P. Liang, V. Pande, and J. Leskovec, “Strategies for pre-training graph neural networks,” in *International Conference on Learning Representations*, 2020. [Online]. Available: <https://openreview.net/forum?id=HJIWWJSFDH>
- [47] S. Brody, U. Alon, and E. Yahav, “How attentive are graph attention networks?” in *International Conference on Learning Representations*, 2021.
- [48] L. Rampášek, M. Galkin, V. P. Dwivedi, A. T. Luu, G. Wolf, and D. Beaini, “Recipe for a general, powerful, scalable graph transformer,” *Advances in Neural Information Processing Systems*, vol. 35, pp. 14 501–14 515, 2022.